تأثير السمك و البيئة الخارجية لدروع الألومنيوم على معدل حدث الأشعة الكونية(الميون) علي مستوي الارض

د. سناء مسعود المختار عبد القادر/جامعة غريان/كلية التربية ككله.
أ. نجاح إبراهيم الحراري/المعهد العالي للعلوم و التقنيات الطبية/ابو سليم.
أ. سمية فرج سعيد تراب/ جامعة الزنتان/كلية تيجي .

الملخص:

جسيمات الأشعة الكونية هي جسيمات الأكثر انتشارًا والتي تصل إلى مستوى الأرض ، لذلك تم إجراء الكثير من الأبحاث حول اكتشافها وقياسها باستخدام أجهزة كشف وطرق مختلفة. ميونات الأشعة الكونية التي تصل إلى مستوى الأرض يمكن أن تعطي معلومات عن التفاعلات الجوية ويمكن أن تشير إلى النشاط الشمسي . تم إجراء هذا البحث لتحقيق الأهداف التالية:

لاكتشاف حدث الميون للأشعة الكونية على مستوى الأرض باستخدام تلسكوب الميون لأنابيب جيجر مولر.

تحديد تأثير الواقيات المصنوعة من الألومنيوم على معدل أحداث ميونات الأشعة الكونية على مستوى الأرض ومن ثم تحديد معامل امتصاصها. تم إجـــراء هذه الدراسة في الطابق الثالث. لاكتشاف أحداث ميونات الأشعة الكونية على مستوى الأرض. الأداة المستخدمة في هذه التجربة هي تلسكوب ميوني لشاشتين للإشعاع لأنابيب جيجر مولر .تم إجـــراء القياس لمدة خمس دقائق. تم إجراء التجربة بزاوية ذروة مع محاذاة الأنابيب المعدلة وراثيًا على طول الاتجاه الشمالي لتحديد تأثير درع الالومنيوم بسماكة مختلفة على معدل حدث الميون للأشعة الكونية على مستوى الأرض. سيتم استخدام طبقة من مادة خفيفة لفصل شاشتي الإشعاع وسيتم وضع تلسكوب الميون تحت طاولة والطبقات المعدنية. في هذا البحث سوف نستخدم عشرين ورقة من الالومنيوم تم تحليل البيانات باستخدام حزم برامج

Effect of thickness and external environment of aluminium shields on the MUON cosmic ray event rate at ground level

SANAA . MASOD . ALMUKHTAR . ABDULQADER/ University of Gharyan/Faculty of Education/ kikla
Najah. Ibrahem .Elharari/Higher Institute of Medical Sciences and Technology / Abu salim
SUMAYA . FARAJ .S . TRAB./ University of Zintan/Faculty of Education /TIGI

ABSTRACT:

In this research, then determine the relationship between the muon events from the vertical direction with the thickness of the aluminium plate on the roof of the third floor. It has coordinates of 101.78 degrees east and 2.92 degrees north and an altitude of 30 m above sea level. The measurement was performed for 5 days which includes 9 sample sets. Aluminium plate with dimensions 10 cm x 10 cm ´ 2 mm, then we increase the number of sheets to twenty. Then the measurements were performed for 9 days comprising 28 sample sets. Its dimensions are 20 cm by 20 cm by 2 mm for aluminium. All measurements were made with an interval of 5 min for each sample using a muon telescope consisting of two RM60 radiation screens containing Geiger-Müller tubes with a 1.6 cm thick separating layer attached to a shell box and the coincidence event either recorded by an LCD monitor. Our measurement shows that the linear increase of absorbance is calculated with the thickness of the lamella in the first 10 and 20 sheets of 10 cm but in the 20 sheets with a decrease of 20 cm. The absorption coefficient (α) of the aluminium sheet shielding thickness was $\alpha = 0.020$. As a result, we found the linear absorption coefficient of aluminium. Thus, in this study, we purposefully used GM tubes to determine the linear mineral absorption coefficient of ground-level cosmic ray muons.

Keywords: MUON**,** Aluminium, absorption coefficient, Thickness, Gamma ray, external environment**,** shields**,** cosmic ray

LIST OF ABBREVIATIONS

μ^- Negative Muon

μ^+ Positive Muon

π^0 Neutral pion

$\pi^{\pm}$Charged pion

γ Gamma ray

$e-$ Electron

$e+$ Positron

ν_μ Muon neutrino

$\overline{\nu_\mu}$ Anti muon neutrino

ν_e Electron neutrino

$\overline{\nu_e}$ Anti electron neutrino

x Thickness of the metal sheets

X total layer thickness

$\mu(X)$ Muon counts at total layer thickness X

N_0 Muon counts when the total layer thickness X=0 at vertical direction ($\theta=0^0$)

α Linear absorption coefficient of the shielding material

Al aluminium shee

1. INTRODUCTION

1.1 BACKGROUND

Every second Earth is being hit by countless sub-atomic particles with various energies from all directions.Those particles are called cosmic rays. About 89% of incoming cosmic ray nuclei are simple protons (hydrogen nuclei), 10% are helium nuclei (alpha particles), and 1% of cosmic ray nuclei are those of the heavier elements. Cosmic rays are usually composed of galactic cosmic rays which originated outside the solar system, through our galaxy. This term also includes particles accelerated in interplanetary space,

and solar energetic particles that are the nuclei and electrons accelerated with energetic events on the sun (Mewaldt 1996).

Cosmic ray particles arrive individually, not in the form of a beam. Upon a particle's arrival into Earth's atmosphere it collides with molecules, mostly with oxygen and nitrogen which results in a cascade of lighter particles which produces so called air showers (Mewaldt 1996).

In 1932, Bruno Rossi, using Geiger tubes and his own invention, the triode coincidence circuit, discovered the presence of highly penetrating and ionizing (i.e. charged) particles in cosmic rays. They were shown in 1936 by Anderson and Nedermeyer to have a mass intermediate between the masses of the electron and the proton. In 1940, Rossi showed that these particles, now called cosmic ray muons, decay in light through the atmosphere with a mean life time in their rest frame of about 2 microseconds. Three years later, using another electronic device of his invention, the time to pulse-height converter (TAC), he measured the mean life of cosmic ray muons at rest in an experiment resembling the present one in Junior Lab, but with Geiger tubes instead of a scintillation detector(Grieder 2001).

Cosmic ray muons are elementary subatomic particles similar to electron but with approximately 200 times greater mass, negative charge and unlike electron limited lifetime, lasting only about 2.2 μs. The symbol for cosmic ray muons is the Greek letter μ−, where the minus sign represents negative charge of the particle.

The cosmic ray muon is able to travel about 10 km from where it is formed in the atmosphere to the ground level. This is a result of relativistic time dilation where the lifetime becomes longer by about 6.6 μs (Grieder 2001).

At ground level, the cosmic ray muon component dominates the flux of particles on the ground at energies above 100 MeV. At lower energies, the cosmic ray muon flux decreases because of their short lifetime but cosmic ray muons with higher energy travel with higher velocities and hence travel longer distances due to the relativistic effects and lose energy due to ionization at a rate of about 2 MeV per g cm^{-2}. Since the column density of our atmosphere is about 1000 g cm^{-2}, a cosmic ray muon loses around 2 GeV of energy, on average, upon reaching the ground (Atri & Melott 2011).

1.2 JUSTIFICATION OF THE RESEARCH

Cosmic ray muon is the most dominant cosmic ray particle that arrives at ground level so a lot of research has been performed on its detection and measurement using various detectors and methods. Cosmic ray muons arriving at ground level can give information on atmospheric interactions and can indicate solar activity (Rebel et al. 2007).

Not many studies on cosmic ray muon arrival have been performed at tropical areas so this research will add more data on cosmic ray muon events at tropical locations. This research will focus on the detection of cosmic ray muons, specifically on the third floor building. Previous research performed in University of Malaysia (UKM) involved studying the effect of building shielding on muon events rate at ground level. This research will show the effect of aluminium shielding on cosmic ray muon event rate at ground level. In this research we use muon telescopes of Geiger-Muller (GM) counters as they are inexpensive, durable, low powered and portable. This will be used to investigate the relationship between absorber materials (atomic number), and their muon absorption coefficients.

2.OBJECTIVES OF THE RESEARCH

This research is carried out with the following objectives:

- To detect cosmic ray muon event at ground level using a muon telescope of Geiger-Muller tubes.
- To determine the effect of aluminium shielding's on the rate of cosmic ray muon events at ground level and then determine their absorption coefficient.

2 .1 COSMIC RAYS

The primary cosmic rays are energetic charged particles that dominantly consist of high energy protons, alpha particles and heavier nuclei. Cosmic ray particles originated from interplanetary space, supernovae explosions and can be generated on the sun. In addition, cosmic rays can be of galactic origins. When cosmic rays get closer to the Earth, they will be affected by the geomagnetic field (Grieder 2001).

Cosmic rays have different origins with various energies. Thus, cosmic rays are classified according to their sources and energies (Dorman 2004):

- Extragalactic cosmic rays are cosmic ray particles with energies up to 10^{21} eV that were generated in radio galaxies, quasars and other objects. These cosmic rays come through intergalactic space to our galaxy until they reach the Earth's atmosphere.
- Galactic cosmic rays are particles with energies at least up to 10^{16} eV and generated in supernova or in magnetospheres of pulsars and double stars. Galactic cosmic rays are also generated by shock waves in interstellar space. This type of cosmic ray is also generated in our galaxy and passes through the heliosphere to reach Earth.
- Solar cosmic rays are cosmic particles with energies up to 15-30 GeV and generated in the solar corona. Thus they are internal relative to the Sun's corona and external for interplanetary space and the Earth's magnetosphere.
- Interplanetary space cosmic rays are cosmic ray particles with energies up to 10-100 MeV and generated by terminal shock waves at the boundary of the heliosphere and by powerful interplanetary shock waves.
- Magnetospheric or planetary cosmic rays are cosmic ray particles with energies up to 10 MeV for Jupiter and Saturn and up to 30 keV for the Earth. They are generated inside the magnetospheres of rotating magnetic planets (Dorman 2004).

2.2 History of Cosmic Ray Research

Cosmic rays were discovered in 1912 by Victor Hess during his experiment in a balloon at high altitudes of about 5 km. He discovered that instead of decreasing the ionization of the air increases with altitude. Beyond that he noticed that there were radiations of very high penetrating power entering the Earth's atmosphere from above (Stanev 2003). This discovery marked the birth of a new field of research cosmic ray physics. For the first half of the 20th century, cosmic rays and their interactions became the only possible means of studying particle physics. After that, important discoveries made by cosmic ray physicists include the discovery of antimatter in the form of the positron by Anderson in 1932. In addition, the discovery of cosmic ray muon, as a heavier version of electron, was made by Neddermeyer and Anderson in 1937. For their important discoveries in cosmic ray physics, Hess and Anderson were awarded a shared Nobel prize in Physics in 1936 (Stal 2005).

2.3 METALS AND MUON ABSORPTION

Metals are sometimes described as an arrangement of positive ions surrounded ability by electrons. There are many kind of metals but my research only will use one kind, a post transition metal of aluminium (Al).

2.3. 1 Aluminum

Aluminum or aluminum (US English) is a silvery white member of the boron group of chemical elements. It has the symbol Al, and its atomic number is 13. Aluminum is the third most abundant element (after oxygen and silicon), and the most abundant metal, in the Earth's crust. The chief ore of aluminum is bauxite. Aluminum is remarkable for the metal's low density at 2.7×10^{3} kgm^{-3} and for its ability to resist corrosion due to the phenomenon of passivation. Aluminum is a soft, durable, lightweight, ductile and malleable metal with appearance ranging from silvery to dull gray, depending on the surface roughness. This allows excellent impact absorption and lower imposed stress levels from structural flexing. The Young's modulus for aluminium is a third that of steel (E = 70,000 MPa). This means that the moment of inertia has to be three times as great for an aluminium extrusion to achieve the same deflection as a steel profile (Federico1985). Figure 1.shows the picture of a few aluminium sheets.

Figure 1. picture of aluminium sheet

2.3.2muon detectors

There are many devices to detect cosmic ray particles, in particular muons. Here we will review the muon detectors of Cherenkov detector, Geiger Muller tubes and BESS (Balloon-borne Experiment with a Superconducting Spectrometer).

2.3.3 Cherenkov Detector

A Cherenkov detector relies on the Cherenkov radiation effect which is the light produced when a charged particle passes through a medium with speed

greater than the speed of light specific to that medium. The particle polarizes the molecules of the medium resulting in emission of radiation (Hsieh et al. 2004). The threshold energy for the emission of the Cherenkov radiation depends on the value of the refraction index of the medium (Stanev 2003).

The most common and efficient Cherenkov detector uses the tank of pure water surrounded by photomultipliers because the refraction index of water is large at about 1.33 and the threshold energy is small. Cherenkov detectors are used to detect extensive air shower particles where these particles move with velocities greater than the speed of light in the atmosphere as a medium. With enough observation and the use of two or three different media, the direction, energy, and possibly the type of particle can be deduced (Kitchin 1984).

2.3.4 Geiger-Muller Counter

The Geiger-Muller (GM) tube was used as a radiation counter in 1908 at Manchester

University by Hans Geiger and Ernest Marsden and later improved by Walther Muller. Figure 2. illustrates the Geiger-Muller tube.

Figure 2. Geiger-Muller Tube.Source: Hudoba 2010

The GM tube or Geiger counter is still an important device for radiation detection. A Geiger counter is known as a gas filled ionization detector. Basically, a Geiger counter consists of two electrodes where there is a potential difference between them. The two electrodes are designed as the outer wall (cathode) and as a central coaxial wire (anode). The gas that filled the tube is argon at a low pressure with a little organic gas (Kitchin 1984).

When an ionizing particle passes through the tube, the gas becomes ionized and the electrons are accelerated toward the central electrode by the external

potential so they begin travelling across the tube. As the ionization level increases, the number of electrons increases to create the current. The current will make a power peak on the register, which are counted and converted to an audible click. Figure 3. shows the principle of the GM tube (Hudoba 2010). The Geiger counter has a disadvantage in that it responds to one event leaving the detector inoperative for a short interval of time which is called the dead time. Because of dead time the detector is not sufficient to cause a second avalanche of electrons (Kitchin 1984).

In addition, the Geiger counter cannot determine the energy loss and momentum and it is not precise. On the other hand, the Geiger counter is the easiest way to detect charged particles. It is inexpensive, low-powered durable and easily portable. To detect cosmic ray particles one can build a cosmic ray telescope of two or three Geiger-Muller counters (GM tubes). The telescope of GM tubes is also used to detect muons and it is called the muon telescope (Brancus et al. 2003).. Since the Geiger-Muller counter is not precise, the muon telescope of Geiger-Muller counters (GM tubes) cannot detect 100% of muons.

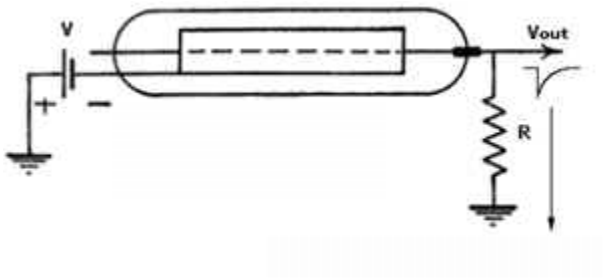

Figure 3. A typical Arrangement for a Geiger Counter
Source: Hudoba 2010

2.3.5bess detector

The BESS (Balloon-borne Experiment with a Superconducting Spectrometer) detector is a high-resolution spectrometer with a large acceptance to perform highly sensitive searches for rare cosmic-ray components, and precise measurement of the absolute fluxes of various cosmic ray (Sanuki et al 2002). The BESS detector is designed inside a cylinder which consists of the following components:

a) Time of flight in the top and bottom (TOF) scintillators which are also used to measure the energy of the particle.

b) Cherenkov counters which is located under the top of time of flight (TOF).
c) Two inner drift chambers (IDC) which are mounted inside the magnetic field space.
d) In the central region, a uniform magnetic field is provided by a thin superconducting solenoid coil. The magnetic-rigidity of an incoming charged particle is measured by a tracking system, which consists of a jet-type drift chamber (JET) and measures up to 28 particle positions.
These detectors provide the multiple measurements for all parameters needed for the reconstruction of the particle energy, mass and charge (Stanev 2004).

3.MATERIAL AND METHOD

This chapter will cover the material and equipment, experimental methodology and data analysis used in this research.

3.1 MATERIAL

The equipment used in this research consists of the RM60 radiation monitor, coincidence box (C-box), LCD-60 display module, and sheet of aluminium.

3.1.1 Radiation Monitor

In this research, the RM60 radiation monitor produced by Aware Electronics(www.aww-el.com)is used to detect cosmic ray muons. Figure 4. shows the RM60 radiation monitor.

Figure 4. The RM60 Radiation Monitor

The RM60 radiation monitor contains a LND712 Geiger-Muller (GM) tube. The window of the GM tube has an areal density of 1.5 to 2.0 mg/cm^2, effective diameter of 9.14 mm (0.360 inch) and effective area of 65.61 mm^2 (0.102 inch^2). The wall of the radiation monitor has a thickness of 0.381 mm (0.012 inch), and effective length of 38.1 mm (1.5 inch). Figure 5. shows the diameter and the length of the LND712 GM tube produced by LND Inc (www.lndinc.com).

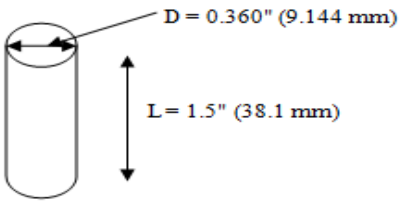

Figure 5. The Geometrical Dimensions of the LND 712 GM tube used in the RM60 Radiation Monitor

Two of the RM60 radiation monitor units were used to make a cosmic ray muon telescope (MT) and connected to a LCD-60 display module with battery of 9 V. Acosmic ray muon telescope can detect muon events or coincidence where coincidence means that the radiation events occur simultaneously in both RM60s determined by a coincidence box (C-box). In addition, we use a separation distance of l between the two radiation monitors, resulting in a smaller solid angle of $\Delta\Omega$. This results in a lower event rate with the angle becomes more defined; i.e $\Delta\theta$ is smaller (less uncertainty) for the arrival direction of the cosmic ray muon events. Figure 6. shows a schematic diagram of the cosmic ray muon telescope comprising of two GM tubes (RM60s) separated by a distance of l=1.6 cm, where a = 0.9 cm and b = 0.5 cm are the distances of the GM tubes from the radiation monitor box upper and lower edges, respectively.

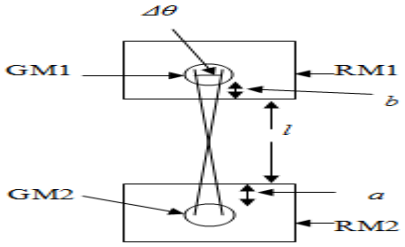

Figure 6. Schematic Diagram of a cosmic ray muon telescope of GM tubes

3.1.2 Coincidence Box

The coincidence box (C-box) produced by Aware Electronic is used to give out a signal when the two radiation monitors register simultaneous radiation events (Figure7). It is connected to the two RM60 radiation monitors by RJ-45 telephone cables to make the cosmic ray muon telescope.

Monitor7. The Coincidence Box (C-box)

3.1.3 LCD 60 Display Module

The LCD-60 Display Module produced by Aware Electronics (www.aw-el.com) is used to display the output signal of the coincidence box to indicate a cosmic ray muon event. The LCD-60 is used to display the count of cosmic ray muon events within a time period. It has two digit readouts. One readout shows counts per minute or counts per second and the other readout displays total counts. It is often useful to have the ability to separate the readout from the sensor unit with the snap in telephone wire. Figure 8. shows the LCD-60 Display Module.

3.1.4 Aluminium Sheet.

Aluminium sheet metal was used as an absorbent or protective material in this study. The aluminium sheets used have a different thickness of 2 mm. At first we use ten aluminium sheets with dimensions of 10 cm x 10 cm x 2 mm, then we increase the number of sheets to 20. Then we use twenty sheets of aluminium sheets with a layer size of 20 cm x 20 cm x 2 mm.

Figure 9 .picture of aluminium sheet

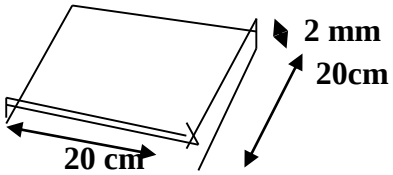

Figure 10. dimension of aluminium sheet

3.1.5 Holding Box

A holding box was fabricated to the GM telescope and place the metal sheets (Figure 11 a.b). The holding box is made of Perspex plastic with dimension 10 cm × 9 cm ×14 cm. The GM telescope is placed inside the holding box and the metal sheets are placed at the top of the holding box. The holding box is strong enough to carry the weight of the metal sheets.

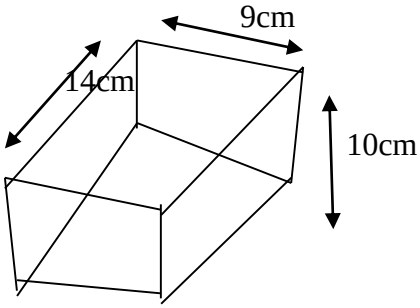

Figure 11b .dimension of holding bo

Figure 11a .picture of holding box

3.2 Measuring method

The experiment was conducted to measure muon events of cosmic rays at ground level on the third floor (top of the roof). The experiment site is located at 101.78°E and 2.92°N and an altitude of 30m. Previous studies of muons were conducted at ground level within the third floor. Which contains the roof

and the protective wall. This research focused on the effect of aluminium shields on the muon event rate of cosmic rays at the ground level.

This study was designed to investigate the effect of aluminium plates on the event rate of cosmic ray muons at ground level using a muon telescope of two RM60 radiators (containing GM tubes) with an interval of l = 1.6 cm to produce a solid angle more specific to the direction of arrival of the muon. This paper focuses on muon events through mineral layers of different thicknesses.

Muon telescopes were standardized vertically, i.e., with a peak angle of θ = 0º with a number of standardized five-minute muon events for the sampling periods recorded on the 60 LCD display. Figure 12. shows a schematic diagram of the experimental setup using RM1 and RM2, two RM60 radiation monitors containing tubes Jaeger Muller. GM1 and GM2 are genetically modified tubes that use the RM 60 radiation monitor to produce the radioactive events RE1 and RE2. The outputs of RE1 and RE2 are connected to the coincidence box CB and produce a muon event ME1.

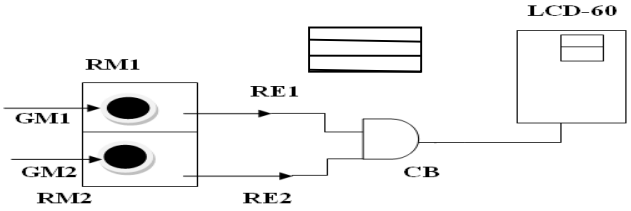

Figure 12 .Schematic diagram of the experimental set up with RM1 and RM2 the two RM60 radiation monitors containing the Geiger-Muller tubes of GM1 and GM2.

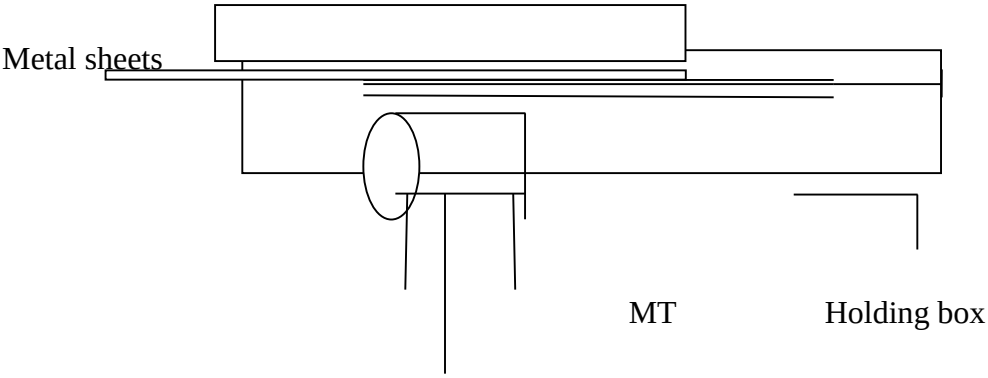

MT

Figure 13a Schematic dimension of the Muon Telescope experimental set up.

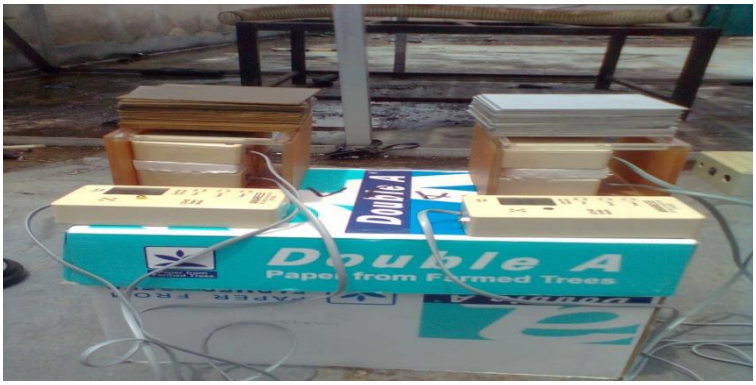

Figure 13b photograph of the Muon Telescope experimental set up.

3.3 Measuring Muon Events Through Aluminium Sheet

In the muon study, a number of metal plates were made on a different number of aluminium plates, which consist of 10 cm x 10 cm x 2 mm of aluminium and then the number of plates was increased to twenty. Then we used twenty aluminium sheets of a larger size. The size of the aluminium is 20 cm by 20 cm by 2 mm. The observation was at the same point on each sheet with a time interval of 5 min, the muon number changes through the aluminium sheets which is related to the thickness of the sheets. For this measurement, we'll start with no layer and then add 2 sheets of up to 10 sheets, then 20 sheets. It is the changes in the rate of muon counting on the sheets that can be used to provide the relationship between the muon number and the thickness of each sheet through the absorption coefficient of the layer thickness for the muon number. The muon telescope was directed in the vertical directions where (θ = 00). When the muon passes through both radiation monitors, this will determine the direction of the muon, and the size and distance of each detector will determine the solid angle of the telescope.

3.4 Data Analysis

Cosmic ray muon data analysis is performed using MS Excel 2007 and MATLAB. The data analysis can be divided into two stages, namely, separation thickness analysis and angle control analysis. MS Excel will be used to analyze the raw data for the different separation number of cosmic ray

muons and then the thickness of the different aluminium sheets. In addition, the performance of muon telescopes in MT1 and MT2 will be analysed and a t-test will be used to determine where the two muon telescopes perform the same or significantly different performance.

3.5 Muon Telescope Separation thickness of metals

The descriptive statistical parameters of minimum, maximum, median, mode, average and standard deviation were used to summarise and interpret the recorded data. If we have a set of numbers, x_1, x_2, x_3...x_{20} where n is the sample size, the median is the number in the middle of a set of numbers, mode is the most repetitive number in this set. The average denoted by $\bar{x}$ is

$$\bar{x} = \frac{1}{20}\sum_{i=1}^{20} x_i = \frac{1}{20}(x_1 + x_2 + \cdots \ldots x_{20}) \quad (3.2)$$

In addition, the standard deviation is a measure of how widely values are dispersed

from the average value ($\bar{x}$). Standard deviation is denoted by $s_x$and given by

$$s_x = \sqrt{\sum_{i=1}^{20} \frac{(x_i - \bar{x})\text{^}2}{n-1}} \quad (3.3)$$

$$\Rightarrow \Delta x = \frac{s_x}{\sqrt{n}} \quad (3.4)$$

The relation between the muon count rate and separation thickness will determine using linear regression to calculate the slope and intercept and their standard errors.

4. RESULT AND DISCUSSION

4.1 Aluminium sheets

Total layer thickness(mm)

The muon counts for the first 9 sampling set are plotted versus the thickness of layers of aluminium sheet in Figure 14.

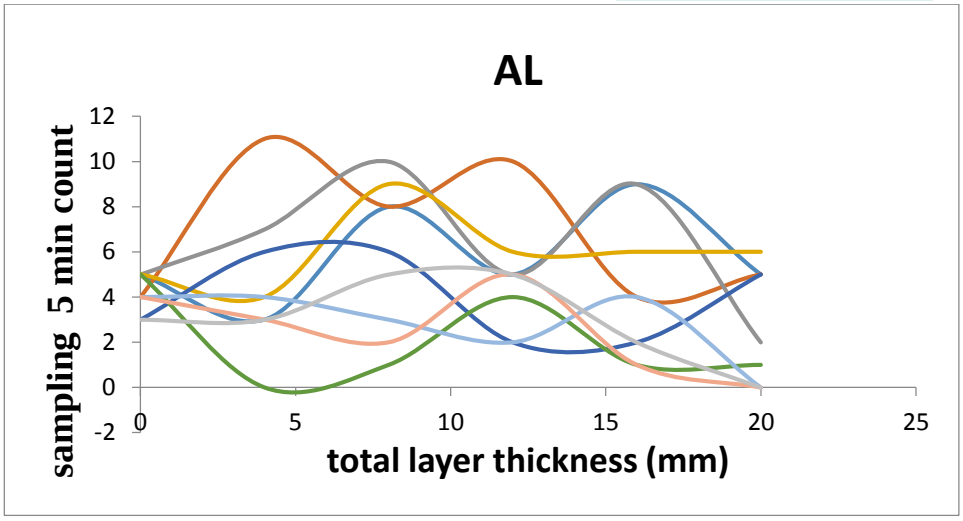

Figure 14. The Muon Counts versus The thickness of layers of aluminium for the first 9 Sampling Sets statistic

4.2 Descriptive statistics of aluminium sheet

The muon counts have been analysed by descriptive statistical for every sheet of aluminium.

		Sheet thickness (mm)					
		0	4	8	12	16	20
1	count	9	9	9	9	9	9
2	Sum	38	41	52	44	38	24
3	Min	3	0	1	2	1	0
4	Max	5	11	10	10	9	6
5	average	4.222	4.556	5.778	4.889	4.222	2.667
6	stdev	0.833	3.127	3.232	2.369	3.153	2.549
7	Cv	0.197	0.686	0.559	0.485	0.747	0.956

	1	2	3	4	5	6
sampling	0	4	8	12	16	20
1	5	3	8	5	9	5
2	4	11	8	10	4	5
3	5	7	10	5	9	2
4	5	4	9	6	6	6
5	3	6	6	2	2	5

		6		5	0	1	4	1	1
		7		4	4	3	2	4	0
		8		4	3	2	5	1	0
		9		3	3	5	5	2	0
8	median	4	4	6	5	4	2		
9	mode	5	3	8	5	9	5		
10	Kurt	-0.501	0.941	-0.258	1.039	0.692	0.129		
11	skew	-1.275	1.629	-1.479	2.438	-1.005	-2.213		
12	range	2	11	9	8	8	6		

We can plot the average of muon counts with the thickness of aluminium sheet. Figure 15. shows how the muon count average changes with the thickness of aluminium sheet.

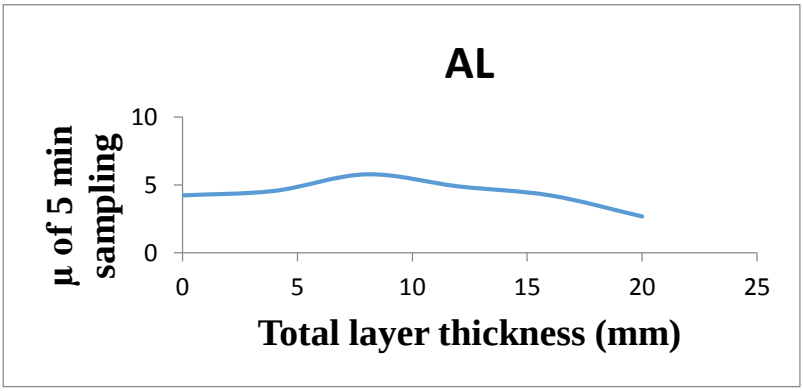

Figure 15. The Average of Muon Counts versus the thickness of aluminium sheet

4.3 Conclusion and discussion

From both of graphs we can see the changes of muon count during the thickness of aluminium sheet. In aluminium sheet the average of muon go up than go down. So the result in these graphs no very well. The measurement will add the layers of aluminium sheets to20 sheets.

Finger 16.

10 cm ×10 cm × 2 mm of aluminium sheet →20 sheets → 13 sampling sets →

4.4. Aluminium sheets

	Total layer thickness(mm)										
	1	2	3	4	5	6	7	8	9	10	11
Sampling	0	4	8	12	16	20	24	28	32	36	40
1	2	2	1	3	3	4	2	1	4	3	2
2	2	4	2	4	6	4	4	3	3	0	2
3	2	4	2	4	4	5	2	3	0	2	4
4	3	3	2	3	0	2	0	2	2	2	1
5	5	3	3	3	4	6	4	2	4	2	2
6	5	3	3	2	1	6	4	0	3	4	2
7	4	5	5	6	2	3	2	6	8	3	6
8	5	3	1	1	3	3	5	4	3	2	3
9	5	5	1	4	1	3	3	6	3	4	2
10	5	1	1	5	5	2	2	4	3	8	4
11	4	1	2	2	5	3	8	3	2	3	2
12	1	1	2	0	2	3	1	6	2	2	3
13	4	3	2	2	5	2	2	4	1	1	1

The muon counts for the first 13 sampling set are plotted versus the total layer thickness of aluminium sheet in Figure 16.

Figure 16. The Muon Counts versus The total layer thickness of aluminium sheet for the first

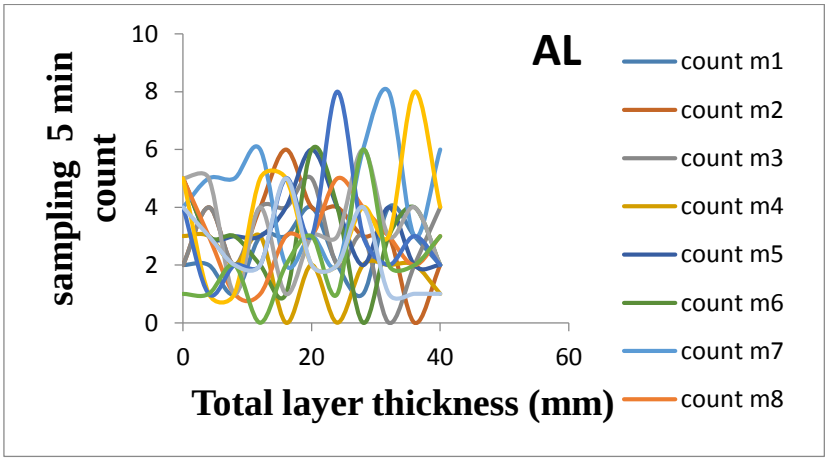

13 Sampling Sets.

4.5 Descriptive statistics of aluminium sheet

The muon counts have been analyzed by descriptive statistical for every sheet of aluminium

We can plot the average of muon counts with the total layer thickness of aluminium sheet. Figure 17. shows how the muon count average changes with the total layer thickness of aluminium sheet.

	0	4	8	12	16	20	24	28	32	36	40
count	13	13	13	13	13	13	13	13	13	13	13
sum	47	38	27	39	41	46	39	44	38	36	34
min	1	1	1	0	0	2	0	0	0	0	1
max	53	5	5	6	6	6	8	6	8	8	6
Average	.615	2.923	2.077	3	3.154	3.385	3	3.385	2.923	2769	2.615
stdev	.4460	1.382	1.115	1.633	1.864	1.391	2.041	1.895	1.891	1.922	1.387
cv	.3999	0.473	0.537	0.544	0.591	0.411	0.680	0.559	0.647	0.694	0.530
median	4	3	2	3	3	3	2	3	3	2	2
mode	5	3	2	3	5	3	2	3	3	2	2
kurt	-0.5	0.166	1.530	-0.196	-0.172	0.784	1.112	-0.059	1.449	1.636	1.269

skew	65-1.218	-0.842	3.191	-0.049	-1.106	-0.421	1.998	-0.591	4.213	4.402	1.781
range	4	4	4	6	6	4	8	6	8	8	5

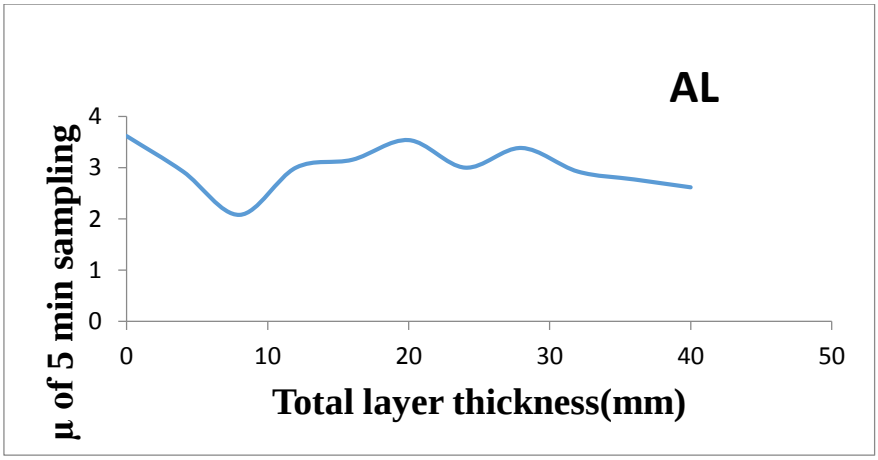

Figure 17. The Average of Muon Counts versus the total layer thickness of aluminium sheet

ln(μ(x))with the total layer thickness (mm) of the aluminium sheet is plotted in Figure 18.

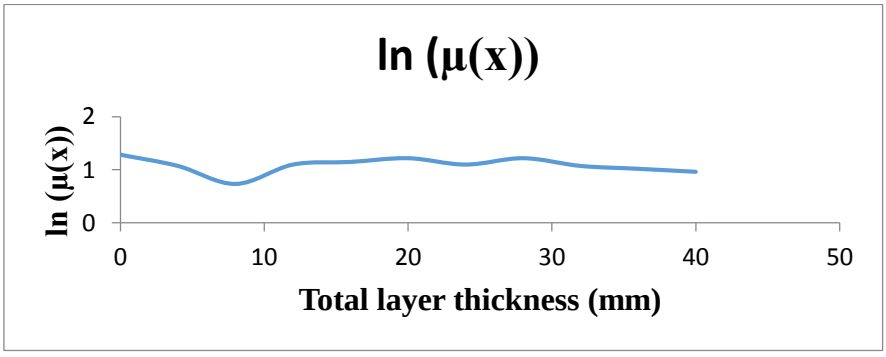

Figure 18. The ln(μ(x)) muon count versus the total layer thickness of aluminium sheet

4.6 Conclusion and discussion

From both graphs we can see the changes in muon number during the thickening of the aluminium. The average muon goes down more. So the result in these graphs is not very good.

The measurement will change the layers of the aluminium sheet to a size of 20 cm by 20 cm.

20 cm × 20 cm × 1.3 mm of copper sheet and 20 cm × 20 cm × 2 mm of aluminium sheet →20 sheets → 28 sampling sets.

4.7 Aluminium sheets

	Total layer thickness (mm)										
	1	2	3	4	5	6	7	8	9	10	11
Sampling	0	4	8	12	16	20	24	28	32	36	40
1	6	5	4	4	4	3	4	1	1	1	0
2	6	6	4	4	3	4	2	3	1	2	1
3	8	6	6	6	3	3	4	2	0	2	1
4	1	2	3	3	1	2	1	1	3	4	2
5	5	2	1	5	4	4	4	2	3	1	0
6	1	1	3	4	3	4	2	2	2	4	2
7	5	4	5	3	5	3	2	1	2	2	2
8	7	2	2	4	2	3	2	5	4	3	2
9	5	7	5	3	4	4	3	3	1	3	1
10	3	3	3	2	5	2	1	3	1	5	4
11	6	4	5	5	5	3	4	5	1	1	3
12	5	3	3	1	5	3	4	5	4	3	2
13	4	4	0	3	2	3	3	2	2	3	4
14	6	3	4	4	2	5	1	3	3	2	1
15	2	2	7	4	5	0	2	1	7	2	1
16	11	3	5	5	2	4	3	0	5	3	1
17	6	11	2	2	1	2	3	3	6	3	2

18	2	3	3	3	5	4	3	4	1	1	3
19	3	2	5	3	5	6	3	2	5	2	3
20	3	3	6	3	1	2	2	0	2	1	2
21	3	6	4	4	1	2	2	5	3	1	3
22	3	4	2	5	5	7	2	3	4	3	3
23	8	8	6	3	6	3	3	1	4	2	4
24	3	3	5	4	5	2	2	2	2	1	2
25	5	5	4	3	4	3	2	1	2	1	0
26	5	3	0	1	2	3	4	4	3	2	3
27	1	3	2	3	2	2	2	2	5	3	3
28	9	6	6	3	3	4	4	3	1	1	0

The muon counts for the first 28 sampling set and μ and σ of 5 min sampling are plotted versus the total layer thickness of aluminum sheet in Figure 19.

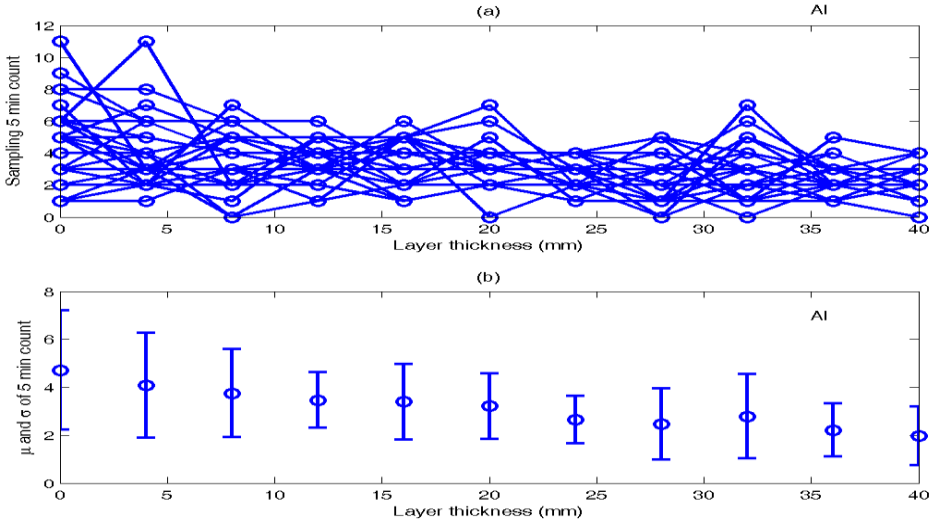

FFigure19. (a) sampling versus the total layer thickness of aluminium sheet(b) average and standard deviation.

4.8 Descriptive statistics of aluminium sheet

	0	4	8	12	16	20	24	28	32	36	40
Count	28	28	28	28	28	28	28	28	28	28	28
Sum	2	4	105	97	95	90	74	69	78	26	25
Minimum	1	1	0	1	1	0	1	0	0	1	0
Maximum	11	11	7	6	6	7	4	5	7	5	4
Average	4.714	4.071	3.750	3.464	3.393	3.214	2.643	2.464	2.786	1.042	1.164
standard deviation	2.492	2.193	1.838	1.170	1.571	1.371	0.989	1.478	1.750	0.201	0.372
Coefficient of Variation	0.529	0.539	0.490	0.338	0.463	0.426	0.374	0.600	0.628	0.192	0.319
Median	5	3	4	3	3.5	3	2.5	2	2.5	2	2
Mode	5	3	5	3	5	3	2	3	1	1	2
Kurt	0.506	1.377	-0.373	-0.132	-0.157	0.606	0.066	-0.297	-0.621	-0.619	-0.056
Skew	0.118	2.368	-0.446	-0.282	-1.388	-1.887	-1.066	-0.661	-0.226	-0.121	-0.836

By using the information above we can plot the average of muon counts and the ln (μ(x)) with the total layer thickness of aluminium sheet. Figure 20. shows how the muon count average changes with the thickness of aluminium sheet.

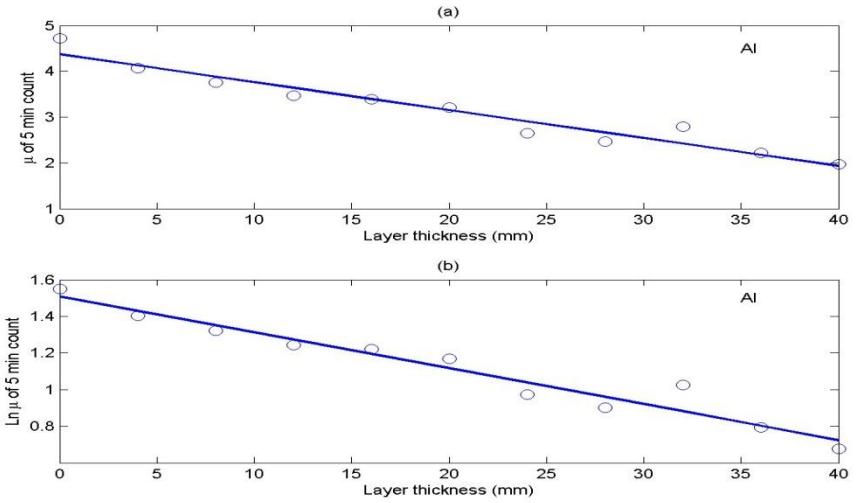

Figure 20. a) Average of Muon Counts
b) ln(μ(x)) versus the total layer thickness of aluminium sheet

The muon counts changes at each sheet of aluminium depended on the total layer thickness of the shielding for each aluminium sheet. From Figure 20. we can see the changes to the average muon counts at the thickness of aluminium sheets:

a) The average muon count decreases with increasing thickness of aluminium sheet, from 0 mm to 28 mm. The highest average muon counts were at 0 mm thickness is because the muon comes in the vertical direction to 0 mm thickness without any shielding from the natural source.
b) From the 28 mm to 32 mm the average muon count increases, then from 32 mm decreases again at the 40 mm.

From the changes of the muon event through the thickness shielding at each sheet of aluminium, we can measure the total layer shielding on muon count by calculating the absorption coefficient (α) with the slope error $\Delta\alpha$ and $\alpha' with\ \Delta\alpha'$

of the aluminium sheet.

From the graphs of aluminium sheet, we can determine the value of the absorption coefficient (α) to be 0.020 mm^{-1}, with the slope error $\Delta\,\alpha\ to\ be$ 0.002mm^{-1} and we can determine the value of the coefficient (α') $to\ be$ 0.061mm^{-1}, with the slope error $\Delta\alpha'$ to be 0.005 mm^{-1}.

4.9 Conclusion and discussion

From graph of aluminium sheet in Figure 20. we can see two distinct regions in the data. Fig(20a), the average muon count is decrease with increasing thickness. Fig(20b), the average muon count increase in a random manner with increasing thickness. The transition from region one and region two occurs around X= 32 mm.

the linear absorption coefficient in aluminium sheet which are

Material	$\alpha \pm \Delta\alpha\ (mm^{-1})$	$\alpha' \pm \Delta\alpha'$ (mm^{-1})
Aluminium sheet	0.020 ± 0.002 10%	0.001 ± 0.005

From the table we can see that, each metal there are $\alpha < \alpha'\ so\ \rightarrow \alpha' \neq \alpha$

Sources of errors and evaluation of results:

a) The muon count was measured during different times daily. This could have affected the muon count values.

b) The muon count could have been influenced by the weather conditions

c) The muon count could have been influenced by the atmospheric pressure and humidity on each sheet of aluminium.

d) The increase of muon count in metals has been influenced by the solid angle.

These factors could have affected the results obtained in this experiment.

5. Conclusion

Muons are the secondary cosmic ray particles and are the most diffuse particles that can be detected at ground level due to relativistic influence. Muon is affected by the geomagnetic field, in particular by the hardness of the geomagnetic pieces. There are many studies of muons in different locations and situations using different equipment. This research is one of the

papers that recorded ground-level muon events in a tropical region. This research was conducted on the third floor (top of the roof). Cosmic ray muons were recorded using two RM60 radiation monitor telescopes containing Geiger-Müller (GM) tubes separated by a layer of 1.6 cm thick polystyrene.

This study was conducted to observe how the muon changes with the thickness of the metal. The metal shield was made of aluminium sheets, and the measurements were measured in muon with a five-minute count with the effective thickness of the shield from two plates to twenty sheets. The difference in thickness leads to changes in the muon number during the metallurgy. The muon was calculated as a function of thickness in terms of the absorption coefficient of the shielding thickness. This research was carried out using the simpler device of Geiger-Muller tubes. GM tube muon telescopes are cheaper than other detectors and less accurate but we have achieved similar results to previous studies using scintillations. It was found that the greater the separation distances, the smaller the muon number, the more decreasing the solid angle of the incident muon. Thus, this research will add more data and information about ground-level muon events in equatorial locations.

5.1 Problems and suggestions for future work

During the experiment, we encountered some difficulties and problems. One such problem is the weather, when it rained the experiment could not be done and then we delayed this after the rain stopped. Another difficulty was that the alignment, or angles, of the muon telescope could not be determined precisely.

Hence, we proposed to automate this experiment so that it can be performed continuously. This will produce more data. In the future, it is expected that the results from monitoring and measuring the muon event will be more accurate and add more information, if an automated system is available to monitor the muon event and also to save time.

REFERENCES

Aguayo, E., Ankney, A.S., Berguson, T.J., Kouzes, R.T., Orrell, J.L., Troy, M.D.
2011. *Cosmic Ray Interactions in Shielding Materials*. Washington: Pacific
North West National Laboratory.

Atri,D. & Melott, A.L. 2011. Modeling high-energy cosmic ray induced terrestrial
muon flux: A lookup table. *Radiation Physics and Chemistry* 80: 701-703.

Bikit , I., Mrda, D.,Anicin, I., Veskovic ,M., Slivka ,J., Krmar , M., Todorovic ,N.,&
Forkapic, S., 2009.Production of X-rays by cosmic-ray muons in heavily shielded
gamma-ray spectrometers. *Nuclear Instruments and Methods in Physics Research A*
606 495–500. University of Belgrade, Studentski Trg 12, 11000 Belgrade, Serbia.

Bonomi,Germano. Donzella,Antonietta.& Zenoni.Aldo. 2010. Muon tomography: the muons and the still mills.

Brancus, I. M., Wentz. J., Mitrica, B., Rebel, H., Petcu, M., Bozodog, H., Mathes, H.
J., Badea, A. F., Bercuci, A., Aiftimiei, C., Duma, M., Meli, A., Toma, G., &
Yulpescu, B. 2003. The east-west effect of the muon charge ratio at energies
relevant to the atmospheric neutrino anomaly. *Nuclear Physics A* 721: 1044c-
1047c.

Enqvist, T., Mattila, A., Fohr, V., Jamsen, T., Lehtola, M., Narkilahti, J.,
Joutsenvaara, J., Nurmenniemi, S., Peltoniemi, J., Remes, H., Sarkamo, J., Shen,
C., & Usoskin, I. 2005. Measurements of muon flux in the Pyhasalmi
underground laboratory. *Nuclear Instruments and Methods in Physics Research*
A 554: 286–290.

Federico M., Mazzolani. 1985. Aluminium alloy structures. *Published by E & FN*
Spon, an imprint of Chapman & Hall, 2-6 Boundary Row, London SE1 8HN, UK.

Fishbine, Brian ,B. 2003. Muon Radiograpy.*Detecting Nuclear Contraband.*

Gilboy,W.B., Jenneson, P.M., & Nayak, N.G. 2005. Industrial Thickness Gauging
With Cosmic- Ray Muons. *Radiation Physics and Chemistry* 74: 454-458.

Grieder,P. K. F. 2001.Cosmic Rays at Earth. Amsterdam: Elsevier.

Hsieh, B., Yu Zhu, G., & Zimmerman, N. 2004. *On the use of a New York city water*
tank as a cosmic ray detector. Department of Electrical Engineering. The
Cooper Union for the Advancement of Science and Art, New York.

Hudoba, G. 2010. *Visualize Particle Radiation in Physics Education*. Hungary: ObudaUniversity.

Kitchin, C. R. 1984. *Astrophysical Techniques*. Bristol: Adam Hilger.

Michael R Moore, Paula Imray, Charles Dameron, Phil Callan, Andrew Langley &Sam
Mangas. 1997. National Environmental Health Forum Monographs Metal Series No.
3. *N a t i o n a l E n v i r o n m e n t a l H e a l t h F o r um.*

Mewaldt, R.A. 1996. Cosmic ray. California Institute of Technology.(online)http://www.srl.caltech.edu/personnel/dick/cos_encyc.html [22-11-2011]

Morenzoni, E., Gl€uckler , H., Prokscha , T., Khasanov , R., Luetkens , H., Birke , M.,
Forgan , E.M., Niedermayer , Ch.,& Pleines, M.2002. Implantation studies of keV
positive muonsin thin metallic layers .*Nuclear Instruments and Methods in Physics Research B 192 254–266.*

Mausumi SenguptaMitra Sarkar , P.K.,& Kudryavtsev , V.A. 2009. Empirical expressions for
angular deviation of muons transmitted through slabs of iron, lead and uranium.
*Nuclear Instruments and Methods in Physics Research A 604 684–693.*University of

Sheffield, S3 7RH, UK

Nagamine, K. 2003. *Introductory Muon Science*. U K: CambridgeUniversityPress.

Rebel, H., Sima, O., Haungs, A., Oehlschläger, J., Manailescu, C., Morariu, C., &

Patrascioiu, A. 2007. *The muon charge ratio in cosmic ray air showers*.

University of Bucharest, Romania.

Santos, J., Augusto, J., Gomes, A., Gurriana, L., Lourenco, N., Maio, A., Marques, C., & Silva, J. 2006. The CRESCERE muon's lifetime experiment. *Current Developments in Technology - Assisted Education* 1322-1326.

Sanuki, T., Fujikawa, M., Abe, K., Anraku, K., Asaoka, Y., Fuke, H., Haino, S.,Imori, M., Izumi, K., Maeno, T., Makida, Y., Matsui, N., Matsumoto, H.,Matsunaga, H., Motoki, M., Nishimura, J., Nozaki, M., Orito, S., Sasaki, M., Shikaze, Y., Sonoda, T., Suzuki, J., Tanaka, K., Toki, Y., Yamamoto, A.,Yamamoto, Y., Yamato, K., Yoshida, T., & Yoshimura, K. 2002. Measurements of atmospheric muon spectra at mountain altitude. *Physics Letters B* 541: 234–242.

Stal,O. 2005.*Detection of Ultra High-Energy Cosmic Particles with the Use of Radioand Radar Methods*. Sweden: Uppsala University.

Stanev, T. 2003. *High Energy Cosmic Rays*. New York: Springer.

Tomono, D., Kojima, T.M., Ishida, K., Ikeda, T., Iwai, Y., Tokuda, M., Kanazawa, Y.,

Matsuda, Y., Matsuzaki, T., Iwasaki, M.,& Yamazaki, Y. 2009. Muon density enhancement with a tapered capillary method. *Physica B 404-577.*

William C., Priedhorsky, Konstantin N., Borozdin, Gary E., Hogan, Christopher Morris,

Alexander Saunders, Larry J., Schultz, & Margaret E. Teasdale. 2003.Detection of high-Z objects using multiple scattering of cosmic ray muons.VOLUME 74, NUMBER 10. *Los Alamos National Laboratory, Los Alamos, New Mexico 87545.*